

Optics Letters

Practical algorithm for custom-made caustic beams

TIMOR MELAMED* AND AMIR SHLIVINSKI

Department of Electrical and Computer Engineering, Ben-Gurion University of the Negev, Beer Sheva, Israel

*Corresponding author: timormel@bgu.ac.il

Received 8 May 2017; accepted 29 May 2017; posted 2 June 2017 (Doc. ID 295338); published 22 June 2017

We present a practical algorithm for designing an aperture field (source) that propagates along a predefined generic beam trajectory that consists of both convex and concave sections. We employ here the mechanism that forms the well-known Airy beam in which the beam trajectory follows a smooth convex caustic of the geometric optics rays and generalize it for a class of beams that are referred to as “caustic beams” (CBs). The implementation is based on “back-tracing” rays from the predefined beam trajectory to the source’s aperture to form its phase distribution. The amplitude is set in order to form a uniform smooth amplitude of the CBs along their trajectories. Several numerical examples are included. © 2017 Optical Society of America

OCIS codes: (080.0080) Geometric optics; (260.1960) Diffraction theory; (080.7343) Wave dressing of rays.

<https://doi.org/10.1364/OL.42.002499>

Designing a beam propagation axis that follows an arbitrary predefined curved trajectory in a homogeneous medium was considered in recent years both theoretically and experimentally in connection with the various types of “accelerating beams,” e.g., Airy beams [1–9] or in a wider perspective in [10–13]. The motivation in using these beams arises mainly from their weakly diffractive *curved* trajectory that is useful in numerous applications such as particle manipulation and optical tweezers [14–16], super-resolution imaging [17,18], plasmon excitation [19,20], and plasma channel generation [21].

A recent study [7] clarified the wave-field mechanism forming the Airy-type beams and demonstrated that it does not adhere to the strict definition of a beam (i.e., a localized wave-field solution that has an evolution along the trajectory dictated by local dynamics), but is the (weakly diffractive) wave-field solution along the smooth convex *caustic* of the geometric optics (GO) rays (see also [22]). Hence, this type of beam can be regarded as a special case of a more generic type of beam which, adopting the notation in [10], is referred to as a “caustic-beam” (CB).

This contribution is aimed at introducing a practical algorithm for designing an aperture field that propagates along a predefined CB trajectory. Noting that the source GO caustic’s

trajectory depends on the *phase distribution* of the aperture source, the proposed implementation is based on “back-tracing” rays from the predefined beam trajectory to the source’s aperture to form its phase distribution. This general framework was also used in [10,11]. The corresponding aperture source *amplitude* can be assigned arbitrarily; however, it can be set in order to give rise to a smooth amplitude caustic.

A general “accelerating beam” has a *convex* trajectory (see, for example, the discussion in [10,11,13]). The algorithm that is presented here can be utilized for designing CBs that meander along complex trajectories that consist of *convex* and *concave* sections. To that end, the source’s phase distribution is set in order to form each of these caustic sections, while the amplitude is set to form a smooth uniform amplitude along the trajectory. An alternative formulation for the design of beam trajectory was reported both theoretically and experimentally in [23,24] for Bessel-type beams. Note that in this latter formulation, each point along the desired trajectory is a focal point of a bundle of rays propagating from subsections of the aperture. The formulation that is presented here utilizes the GO eikonal to give a CB trajectory which is not a focal point, but an envelope of rays (caustic).

Following the introductory discussion, given the generic trajectory in the two-dimensional (2D) domain $[x(s), z(s)]$, with s as a parameter in the interval $s \in [0, s_{\max}]$, we are seeking a practical algorithm for the evaluation of a source (aperture field) that corresponds to a 2D beam-type field whose beam trajectory follows the curved trajectory in free space. The aperture field is of the high frequency (ray-) field of the form

$$u(x_0) = A_0(x_0) \exp[-jkS_0(x_0)], \quad (1)$$

where $k = \omega/c$ is the wavenumber, with c denoting free space wave speed. In Eq. (1), x_0 is the coordinate along the aperture; A_0 and S_0 are identified as the aperture field amplitude and phase distributions, respectively. The algorithm that is presented in this Letter evaluates the two functions, A_0 and S_0 , from the desired trajectory $[x(s), z(s)]$.

First, we discuss beam trajectories that consist of a single convex (or a single concave) curve. We identify the predefined (desired) trajectory, $[x(s), z(s)]$, as a *caustic trajectory*. Therefore, we are seeking an aperture (ray) field that, within GO conventions, radiates ray trajectories that form the desired curved caustic. The envelope of the straight-line ray trajectories

emanating from the $z = 0$ aperture constitutes the caustic trajectory.

Each point $[x(s), z(s)]$ on the caustic trajectory is mapped to the corresponding tangent ray emanating from point $x_0(s)$ and in the direction $\theta_0[x_0(s)]$ from the aperture. Referring to Fig. 1, we identify the tangent ray trajectory emanating from point x_0 as

$$x_0 = -z(s) \cot \theta_0(x_0) + x(s), \quad \cot \theta_0(x_0) = x'(s)/z'(s), \tag{2}$$

where the prime denotes a derivative with respect to the argument. By using Eq. (2), we obtain an interval $[x_0(0), x_0(s_{\max})]$ over the aperture from which the rays that form the caustic are radiated. For each point x_0 in the interval we calculate the corresponding angle $\theta_0(x_0)$ (see Fig. 1). The ray angle $\theta_0(x_0)$ is related to the aperture phase in Eq. (1) via [25]

$$S'_0(x_0) = \cos \theta_0. \tag{3}$$

Referring to Fig. 1, we identify a single interval over the aperture from which the caustic rays are emanating, $x_0 \in [x_0(0), x_0(s_{\max})]$. By using Eq. (2) in Eq. (3), we obtain the desired aperture field phase

$$S_0(x_0) = \int_{x_0(0)}^{x_0} [1 + \tan^2 \theta_0(x'_0)]^{-1/2} dx'_0. \tag{4}$$

The aperture field phase in Eq. (4) gives rise to a CB along the trajectory $[x(s), z(s)]$. For simple caustics, near the caustic trajectory the field is described asymptotically by (see the extended discussion in [26])

$$u(s, n) \sim A_c(s) e^{-jk_s z + j\pi/4} A_i \left(-n \sqrt{\frac{2k^2}{\rho_c(s)}} \right), \tag{5}$$

where $A_i(s)$ denotes the Airy function, (s, n) are the parallel and normal local trajectory coordinates along the caustic, respectively, ρ_c is the radius of curvature of the caustic, and A_c is a reference amplitude on the caustic.

The maxima of the caustic field in Eq. (5) are not obtained over the desired trajectory where $n = 0$, since the Airy function maximum is obtained at $\delta = -1.019$. By using Eq. (5), we obtain the off-axis deviation of the maximum from the beam trajectory, Δ_{\max} , and the CB normal width, $W_n(s)$, in the form

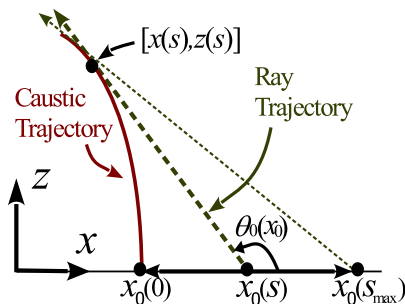


Fig. 1. Single section beam trajectory: for caustic trajectories that are either convex or concave, the aperture rays emanate from a single interval $[x_0(0), x_0(s_{\max})]$ over the aperture. The mapping of $s \rightarrow x_0(s)$ is obtained via Eq. (2).

$$\Delta_{\max}(s) \approx |\delta| k^{-1} \sqrt[3]{k \rho_c(s)/2}, \quad W_n(s) = \delta_n k^{-1} \sqrt[3]{k \rho_c(s)/2}. \tag{6}$$

Here $\delta_n = 1.627$ denotes the Airy function -3 dB width. In the method presented here, the aperture size is adjusted to the predefined trajectory such that no diffraction occurs along the trajectory. Note that the proposed finite-energy beams are diffractionless over a finite distance determined by the predefined trajectory.

We present here two implementations for single section beams: an Airy type and a (half-period) sine trajectory. The aperture fields phases are obtained via Eq. (4). Here the amplitude is taken as a constant over the interval $[x_0(0), x_0(s_{\max})]$ in which the caustic forming rays are emanating; i.e.,

$$A_0(x_0) = \begin{cases} 1 & x_0 \in [x_0(0), x_0(s_{\max})] \\ 0 & \text{elsewhere} \end{cases}. \tag{7}$$

In order to verify the resulting CBs, the $z = 0$ aperture fields are propagated into a $z \geq 0$ half-space via the standard exact *plane wave spectral* representation

$$u(x, z) = \frac{1}{2\pi} \int_{-\infty}^{\infty} U(k_x) \exp[-j(k_x x + k_z z)] dk_x, \tag{8}$$

where $k_z = \sqrt{k^2 - k_x^2}$ with $\text{Re}\{k_z\} \geq 0$ and $\text{Im}\{k_z\} \leq 0$ denotes the longitudinal spectral wavenumber, and

$$U(k_x) = \int_{-\infty}^{\infty} u(x_0) \exp(jk_x x_0) dx_0 \tag{9}$$

is the plane wave spectrum that corresponds to the aperture field $u(x_0)$. Since the aperture field-caustic field relation is linear, we plot in all the following figures the caustic field that is normalized to the mean of its on-axis field. The on-axis field is defined as the maximum (amplitude) field along constant z lines in the (x, z) plane.

The first example is a caustic trajectory of $z/\lambda = \alpha \sqrt{x/\lambda}$, where α is a scaling parameter. This trajectory corresponds to the conventional Airy beam [7]. By setting $\alpha = -3$ and using Eqs. (2)–(4), we obtain the phase functions. By setting the amplitudes according to Eq. (7) and evaluating the propagating fields in the $z \geq 0$ half-space via Eq. (8), we obtain the CB-fields in Fig. 2(a).

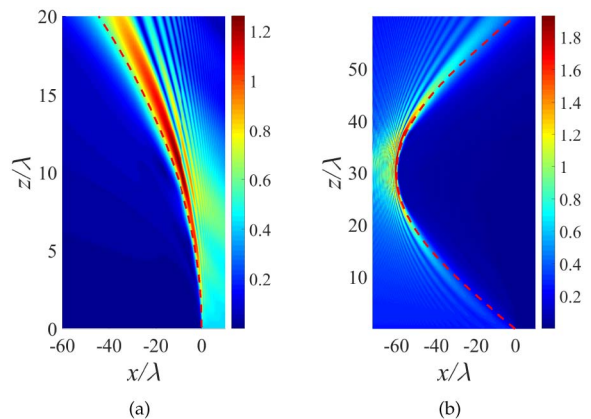


Fig. 2. Single section trajectory. (a) Airy type beam with $\alpha = -3$. (b) Sine trajectory over a half-period. Note that the maxima of the CB deviate from the desired (dashed line) trajectory.

The CB trajectories in Fig. 2 deviate from the desired ones (curved line). According to Eq. (6), this deviation increases as the radius of curvature of the desired beam trajectory increases. In these figures, the radius of curvature increases as z increases.

The second example involves a sine trajectory caustic with $x/\lambda = 60 \sin(\pi z/60\lambda)$ for $z < 60\lambda$. Following a similar procedure, we obtain the CB field in Fig. 2(b). Note that the amplitude of the resulting CB along its trajectory deviates significantly from its maximum value.

The caustic trajectory in Fig. 3 consists of both convex and concave segments. In this case, we map each segment via Eq. (2) to a corresponding interval over the aperture from which the caustic rays are emanating, $x_0 \in [x_0^n(s_0^n), x_0^n(s_0^{n+1})]$. Here $s_0^1 = 0$, and s_0^n are the concave/convex transition points over the trajectory. Note that the intervals that correspond to the different trajectory segments can overlap to share a common physical aperture, as illustrated in Fig. 3.

By applying the procedure in Eqs. (2)–(4), we evaluate the aperture fields' phases that form each of the caustic segments, $S_n(x_0)$. Thus, the aperture field that forms the entire trajectory is obtained by summing over the fields, i.e.,

$$u(x_0) = \sum_n A_n(x_0) \exp[-jkS_n(x_0)], \quad (10)$$

where the A_n s are the amplitudes of the different sections' intervals [see the discussion preceding Eqs. (7) and (11)].

Next, we evaluate the aperture field that radiates a (one period) sine caustic trajectory. The aperture field phases of each segment were obtained via the algorithm that is given in the previous paragraph, and the amplitudes were set according to Eq. (7). The trajectory $x/\lambda = 60 \sin(\pi z/60\lambda)$ over $0 \leq z \leq 120\lambda$ is plotted in Fig. 4(a). We identify two segments, a concave curve (relative to the z -axis) ranging from $0 \leq z \leq 60\lambda$, and a convex curve (for $60\lambda \leq z \leq 120\lambda$).

The $z = 0$ aperture field is propagated into $z \geq 0$ via Eqs. (8) and (9). The resulting field amplitude is plotted in Fig. 4(a). One can clearly observe that the resulting caustic trajectory follows the desired one. As in Fig. 2(b), the need for adjusting the aperture field amplitude in order to obtain a constant caustic amplitude is clearly identified. This is carried out in Eq. (11).

The inflection point of the CB in Fig. 4(a) forms a bifurcation of the beam trajectory. This is due to the maxima deviation from the caustic trajectory in Eq. (6) that shifts the maxima curve left or right to the trajectory in concave or convex segments, respectively. Note that the deviation in

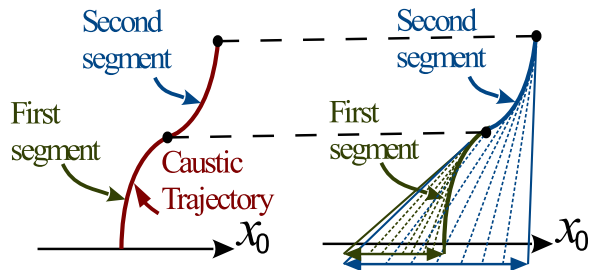


Fig. 3. Multi-segment trajectory. The trajectory consists of (lower) concave and (upper) convex segments with respect to the z -axis. Each of these segments is formed by rays that are emanating from corresponding intervals over the aperture with possible overlaps.

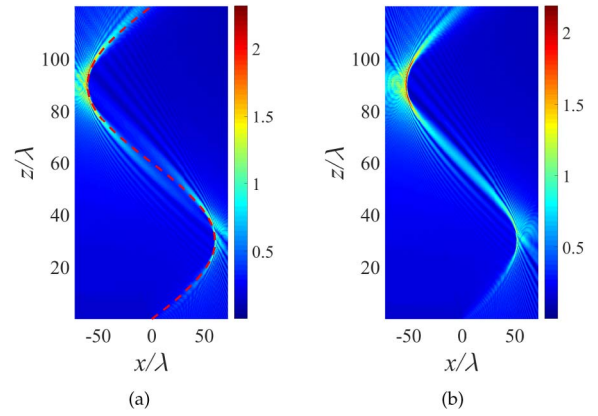


Fig. 4. Multi-segment sine trajectory over one period. (a) Original field in the vicinity of the caustic and (b) the field after applying the shifts to the segment aperture fields in order to obtain a continuous beam trajectory.

Eq. (6) is not valid in the vicinity of the inflection point, since the radius of curvature at that point is infinite.

In order to obtain a single beam trajectory, we shift the constituent field segments in Eq. (10) by the corresponding deviations. This deviation is easily evaluated numerically by sampling the amplitude of the field in Fig. 4(a) over the line $z/\lambda = 60$. The resulting CB is plotted in Fig. 4(b), which demonstrates that the resulting beam maxima trajectory is continuous.

The amplitudes of the caustic fields along the caustic trajectories in all the above examples are clearly not constant. Next, we introduce a practical and simple algorithm that is aimed at adjusting the aperture field amplitude in order to improve the beam field homogeneity along the caustic trajectory. This algorithm can be easily adapted for other specifications that may arise in different applications.

First, we discuss single segment trajectories. In the proposed procedure, we sample the caustic field that was obtained by using the constant aperture amplitude in Eq. (7) along the ray trajectory $[x(s), z(s)]$ and map each point to the corresponding point over the aperture by using the mapping in Eq. (2), $[x_0(0), x_0(s_{\max})]$. Next, we multiply the aperture by the (real) filter

$$F(x_0) = |u_{\max}|/|u[x(s(x_0)), z(s(x_0))]|, \quad (11)$$

where $|u[x(s(x_0)), z(s(x_0))]|$ is the amplitude of the caustic field over the caustic trajectory, and $|u_{\max}|$ denotes its on-axis maximum. The filter in Eq. (11) pre-amplifies the intervals that form the weak amplitude sections of the caustic. On the practical side, spatial light modulators can be used for imprinting a phase profile on an optical beam, as well as to shape its amplitude using the beam polarization.

Figure 5(a) plots the on-axis amplitude of the CB in Fig. 2(b) as a function of z/λ . The figure demonstrates that the peak of the amplitude; about $z/\lambda = 30$ is significantly larger than its minimum at the lower ($0 < z/\lambda < 10$) and upper ($50 < z/\lambda < 60$) parts of the trajectory. The corresponding filter in Eq. (11) as a function of the aperture coordinate x_0 is plotted in Fig. 5(b). The filter amplifies rays that are emanating from the intervals $-20 \leq x_0/\lambda \leq 0$ and

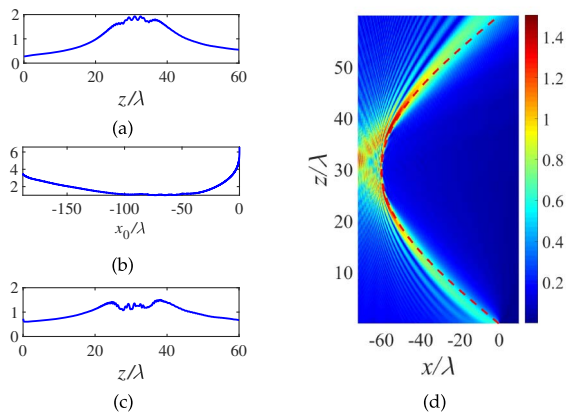


Fig. 5. Adjusting the CB amplitude. (a) On-axis amplitude of the CB in Fig. 2(b), (b) the corresponding pre amplifier filter in Eq. (11), (c) the on-axis amplitude of the pre-amplified CB, and (d) the pre-amplified CB amplitude.

$-200 \leq x_0/\lambda \leq -160$. These aperture intervals form the lower and upper caustic parts in Fig. 2(b), respectively.

The resulting (pre-amplified) CB is plotted in Fig. 5(d), and its corresponding on-axis amplitude is plotted in Fig. 5(c). By comparing the on-axis field in Fig. 5(a) [corresponding to Fig. 2(b)] to the pre-amplified one in Fig. 5(c) [corresponding to Fig. 5(d)], we note that the *pre-amplified* on-axis field is more homogeneous. In order to quantify this inhomogeneity, we calculate the standard deviations of the on-axis fields, after normalizing each to its mean. This criterion is impartial to multiplication by a constant. The standard deviations were calculated to be 0.5 or 0.27 for the constant or pre-amplified fields, respectively. Therefore, we conclude that this process improves the homogeneity of the on-axis caustic field. This process can be repeated at the cost of increasing off-axis zones so the procedure can be stopped pending on the application requirements.

For multi-segment trajectories, we basically repeat the same procedure for each of the segments while keeping the resulting filter continuous. By applying this procedure to the one period sine CB in Fig. 4(b), we obtain the pre-amplified aperture field

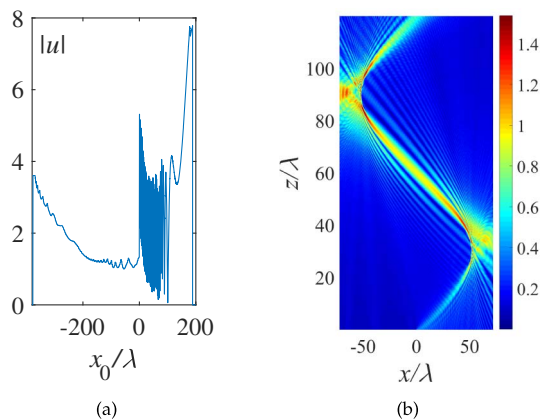


Fig. 6. Adjusting the multi-segment CB amplitude. (a) Amplitude of the pre-amplified aperture field and (b) the corresponding pre-amplified CB amplitude.

in Fig. 6(a). Note that the aperture field amplitude emphasizes the ray tubes that form the lower ($0 < x_0/\lambda < 20$), middle ($150 < x_0/\lambda < 200$), and upper ($-400 < x_0/\lambda < -300$) on-axis fields in Fig. 4(b).

The corresponding pre-amplified caustic field is plotted in Fig. 6(b). By comparing this figure to Fig. 4(b) we conclude that the pre-amplified on-axis CB is more homogeneous than the constant amplitude one. The standard deviation of the normalized on-axis fields, which are 0.47 or 0.27 for the constant or pre-amplified fields, respectively, support this conclusion.

In this Letter, a practical algorithm for the construction of the aperture field distribution that corresponds to a (pre-defined) custom-made 2D CB is presented. The procedure involves the construction of the aperture source phase and amplitude distributions. Numerical examples demonstrate the efficiency of the algorithm to calculate the desired source for complex beam trajectories that consist of both convex and concave sections. This Letter can be extended to include generic three-dimensional beam trajectories (see, e.g., [9]) that are characterized by curvature and torsion.

REFERENCES

- G. A. Siviloglou, J. Broky, A. Dogariu, and D. N. Christodoulides, *Phys. Rev. Lett.* **99**, 213901 (2007).
- G. A. Siviloglou and D. N. Christodoulides, *Opt. Lett.* **32**, 979 (2007).
- I. M. Besieris and A. M. Shaarawi, *Opt. Lett.* **32**, 2447 (2007).
- J. Broky, G. A. Siviloglou, A. Dogariu, and D. N. Christodoulides, *Opt. Express* **16**, 12880 (2008).
- G. A. Siviloglou, J. Broky, A. Dogariu, and D. N. Christodoulides, *Opt. Lett.* **33**, 207 (2008).
- M. A. Bandres, *Opt. Lett.* **34**, 3791 (2009).
- Y. Kaganovsky and E. Heyman, *Opt. Express* **18**, 8440 (2010).
- Y. Hu, G. A. Siviloglou, P. Zhang, N. K. Efremidis, D. N. Christodoulides, and Z. Chen, in *Nonlinear Photonics and Novel Optical Phenomena*, Z. Chen and R. Morandotti, eds. (Springer, 2012), pp. 1–46.
- Y. Kaganovsky and E. Heyman, *J. Opt. Soc. Am. A* **29**, 671 (2012).
- L. Froehly, F. Courvoisier, A. Mathis, M. Jacquot, L. Furfaro, R. Giust, P. A. Lacourt, and J. M. Dudley, *Opt. Express* **19**, 16455 (2011).
- E. Greenfield, M. Segev, W. Walasik, and O. Raz, *Phys. Rev. Lett.* **106**, 213902 (2011).
- N. K. Efremidis and D. N. Christodoulides, *Opt. Lett.* **35**, 4045 (2010).
- P. Zhang, Y. Hu, T. Li, D. Cannan, X. Yin, R. Morandotti, Z. Chen, and X. Zhang, *Phys. Rev. Lett.* **109**, 193901 (2012).
- J. Baumgartl, M. Mazilu, and K. Dholakia, *Nat. Photonics* **2**, 675 (2008).
- D. N. Christodoulides, *Nat. Photonics* **2**, 652 (2008).
- Z. Zheng, B.-F. Zhang, H. Chen, J. Ding, and H.-T. Wang, *Appl. Opt.* **50**, 43 (2011).
- S. Jia and X. Zhuang, *Opt. Photon. News* **25**, 35 (2014).
- S. Jia, J. C. Vaughan, and X. Zhuang, *Nat. Photonics* **8**, 302 (2014).
- D. Kuang, Y. Cao, T. Lépine, and W. Mi, *IEEE Photon. J.* **7**, 6 (2015).
- A. E. Minovich, A. E. Klein, D. N. Neshev, T. Pertsch, Y. S. Kivshar, and D. N. Christodoulides, *Laser Photon. Rev.* **8**, 221 (2014).
- P. Polynkin, M. Kolesik, J. V. Moloney, G. A. Siviloglou, and D. N. Christodoulides, *Science* **324**, 229 (2009).
- S. Vo, K. Fuerschbach, K. P. Thompson, M. A. Alonso, and J. P. Rolland, *J. Opt. Soc. Am. A* **27**, 2574 (2010).
- I. D. Chremmos, Z. Chen, D. N. Christodoulides, and N. K. Efremidis, *Opt. Lett.* **37**, 5003 (2012).
- J. Zhao, P. Zhang, D. Deng, J. Liu, Y. Gao, I. D. Chremmos, N. K. Efremidis, D. N. Christodoulides, and Z. Chen, *Opt. Lett.* **38**, 498 (2013).
- M. Born and E. Wolf, *Principles of Optics* (Pergamon, 1964).
- D. Ludwig, *Commun. Pure Appl. Math.* **19**, 215 (1966).